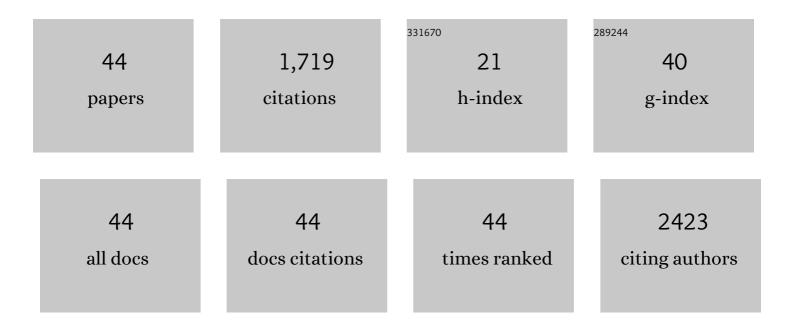
## **Buck E Rogers**

List of Publications by Year in descending order

Source: https://exaly.com/author-pdf/1527795/publications.pdf Version: 2024-02-01



#	Article	IF	CITATIONS
1	Dendritic Cell Paucity Leads to Dysfunctional Immune Surveillance in Pancreatic Cancer. Cancer Cell, 2020, 37, 289-307.e9.	16.8	252
2	Agonism of CD11b reprograms innate immunity to sensitize pancreatic cancer to immunotherapies. Science Translational Medicine, 2019, 11, .	12.4	148
3	MicroPET Imaging of a Gastrin-Releasing Peptide Receptor-Positive Tumor in a Mouse Model of Human Prostate Cancer Using a 64Cu-Labeled Bombesin Analogue. Bioconjugate Chemistry, 2003, 14, 756-763.	3.6	138
4	Copper import in Escherichia coli by the yersiniabactin metallophore system. Nature Chemical Biology, 2017, 13, 1016-1021.	8.0	112
5	AKT Inhibitors Promote Cell Death in Cervical Cancer through Disruption of mTOR Signaling and Glucose Uptake. PLoS ONE, 2014, 9, e92948.	2.5	68
6	Molecular Imaging of Gastrin-Releasing Peptide Receptor-Positive Tumors in Mice Using <sup>64</sup> Cu- and <sup>86</sup> Y-DOTAâ^'(Pro <sup>1</sup> ,Tyr <sup>4</sup> )-Bombesin(1â^'14). Bioconjugate Chemistry, 2007, 18, 724-730.	3.6	65
7	Radiation-induced neoantigens broaden the immunotherapeutic window of cancers with low mutational loads. Proceedings of the National Academy of Sciences of the United States of America, 2021, 118, .	7.1	62
8	Evaluation of [89Zr]trastuzumab-PET/CT in differentiating HER2-positive from HER2-negative breast cancer. Breast Cancer Research and Treatment, 2018, 169, 523-530.	2.5	59
9	Myocardial B cells are a subset of circulating lymphocytes with delayed transit through the heart. JCI Insight, 2020, 5, .	5.0	57
10	Enhancing the anti-tumour activity of 177Lu-DOTA-octreotate radionuclide therapy in somatostatin receptor-2 expressing tumour models by targeting PARP. Scientific Reports, 2020, 10, 10196.	3.3	54
11	Evaluation of <sup>64</sup> Cu-Based Radiopharmaceuticals that Target Aβ Peptide Aggregates as Diagnostic Tools for Alzheimer's Disease. Journal of the American Chemical Society, 2017, 139, 12550-12558.	13.7	53
12	Amphiphilic Distyrylbenzene Derivatives as Potential Therapeutic and Imaging Agents for Soluble and Insoluble Amyloid β Aggregates in Alzheimer's Disease. Journal of the American Chemical Society, 2021, 143, 10462-10476.	13.7	51
13	Targeted radiotherapy with [90Y]-SMT 487 in mice bearing human nonsmall cell lung tumor xenografts induced to express human somatostatin receptor subtype 2 with an adenoviral vector. Cancer, 2002, 94, 1298-1305.	4.1	42
14	In Vitro and In Vivo Evaluation of a 64Cu-Labeled Polyethylene Glycol-Bombesin Conjugate. Cancer Biotherapy and Radiopharmaceuticals, 2004, 19, 25-34.	1.0	42
15	Copper-64 radiolabeling and biological evaluation of bifunctional chelators for radiopharmaceutical development. Nuclear Medicine and Biology, 2012, 39, 1099-1104.	0.6	42
16	Metal-chelating benzothiazole multifunctional compounds for the modulation and <sup>64</sup> Cu PET imaging of Al² aggregation. Chemical Science, 2020, 11, 7789-7799.	7.4	40
17	MicroPET imaging of gene transfer with a somatostatin receptor-based reporter gene and (94m)Tc-Demotate 1. Journal of Nuclear Medicine, 2005, 46, 1889-97.	5.0	38
18	Injectable Hydrogels for Localized Chemotherapy and Radiotherapy in Brain Tumors. Journal of Pharmaceutical Sciences, 2018, 107, 922-933.	3.3	35

**BUCK E ROGERS** 

#	Article	IF	CITATIONS
19	Nuclear Uptake and Dosimetry of 64Cu-Labeled Chelator Somatostatin Conjugates in an SSTr2-Transfected Human Tumor Cell Line. Journal of Nuclear Medicine, 2007, 48, 1390-1396.	5.0	28
20	Design of a multivalent bifunctional chelator for diagnostic <sup>64</sup> Cu PET imaging in Alzheimer's disease. Proceedings of the National Academy of Sciences of the United States of America, 2020, 117, 30928-30933.	7.1	25
21	Glutaminase Inhibitors Induce Thiol-Mediated Oxidative Stress and Radiosensitization in Treatment-Resistant Cervical Cancers. Molecular Cancer Therapeutics, 2020, 19, 2465-2475.	4.1	25
22	Intraperitoneal Radioimmunotherapy with a Humanized Anti-TAG-72 (CC49) Antibody with a Deleted CH2 Region. Cancer Biotherapy and Radiopharmaceuticals, 2005, 20, 502-513.	1.0	23
23	Tumor localization of a radiolabeled bombesin analogue in mice bearing human ovarian tumors induced to express the gastrin-releasing peptide receptor by an adenoviral vector. Cancer, 1997, 80, 2419-2424.	4.1	21
24	Characterization of Somatostatin Receptor Subtype 2 Expression in Stably Transfected A-427 Human Cancer Cells. Molecular Imaging, 2007, 6, 7290.2007.00001.	1.4	21
25	Metabolically Stabilized <sup>68</sup> Ga-NOTA-Bombesin for PET Imaging of Prostate Cancer and Influence of Protease Inhibitor Phosphoramidon. Molecular Pharmaceutics, 2016, 13, 1347-1357.	4.6	21
26	Evaluation of copper-64-labeled somatostatin agonists and antagonist in SSTr2-transfected cell lines that are positive and negative for p53: implications for cancer therapy. Nuclear Medicine and Biology, 2012, 39, 187-197.	0.6	20
27	Novel Structural Modification Based on Evans Blue Dye to Improve Pharmacokinetics of a Somastostatin-Receptor-Based Theranostic Agent. Bioconjugate Chemistry, 2018, 29, 2448-2454.	3.6	20
28	Copper-67-Labeled Bombesin Peptide for Targeted Radionuclide Therapy of Prostate Cancer. Pharmaceuticals, 2022, 15, 728.	3.8	17
29	Amyloid β-Binding Bifunctional Chelators with Favorable Lipophilicity for <sup>64</sup> Cu Positron Emission Tomography Imaging in Alzheimer's Disease. Inorganic Chemistry, 2021, 60, 12610-12620.	4.0	15
30	Matched-pair, 86Y/90Y-labeled, bivalent RGD/bombesin antagonist, [RGD-Glu-[DO3A]-6-Ahx-RM2], as a potential theranostic agent for prostate cancer. Nuclear Medicine and Biology, 2018, 62-63, 71-77.	0.6	14
31	Positron-emission tomography (PET) imaging agents for diagnosis of human prostate cancer: agonist vs. antagonist ligands. In Vivo, 2012, 26, 583-92.	1.3	14
32	PEGylated peptide to TIP1 is a novel targeting agent that binds specifically to various cancers in vivo. Journal of Controlled Release, 2019, 298, 194-201.	9.9	13
33	Preclinical Evaluation of an Engineered Single-Chain Fragment Variable-Fragment Crystallizable Targeting Human CD44. Journal of Nuclear Medicine, 2021, 62, 137-143.	5.0	13
34	Practical considerations for quantitative clinical SPECT/CT imaging of alpha particle emitting radioisotopes. Theranostics, 2021, 11, 9721-9737.	10.0	12
35	Novel hexadentate and pentadentate chelators for 64Cu-based targeted PET imaging. Bioorganic and Medicinal Chemistry, 2014, 22, 2553-2562.	3.0	9
36	Development of a Radiolabeled Irreversible Peptide Ligand for PET Imaging of Vascular Endothelial Growth Factor. Journal of Nuclear Medicine, 2014, 55, 1029-1034.	5.0	8

BUCK E ROGERS

#	Article	IF	CITATIONS
37	Structure-activity relationship studies and bioactivity evaluation of 1,2,3-triazole containing analogues as a selective sphingosine kinase-2 inhibitors. European Journal of Medicinal Chemistry, 2020, 206, 112713.	5.5	8
38	2-(4-Hydroxyphenyl)benzothiazole dicarboxylate ester TACN chelators for <sup>64</sup> Cu PET imaging in Alzheimer's disease. Dalton Transactions, 2022, 51, 1216-1224.	3.3	8
39	Neutral Ligands as Potential <sup>64</sup> Cu Chelators for Positron Emission Tomography Imaging Applications in Alzheimer's Disease. Inorganic Chemistry, 2022, 61, 4778-4787.	4.0	8
40	<sup>68</sup> Ga-Labeled Benzothiazole Derivatives for Imaging AÎ <sup>2</sup> Plaques in Cerebral Amyloid Angiopathy. ACS Omega, 2022, 7, 20339-20346.	3.5	6
41	Aerosol-synthesized siliceous nanoparticles: impact of morphology and functionalization on biodistribution. International Journal of Nanomedicine, 2018, Volume 13, 7375-7393.	6.7	5
42	Radiolabeled 6-(2, 3-Dichlorophenyl)-N4-methylpyrimidine-2, 4-diamine (TH287): A Potential Radiotracer for Measuring and Imaging MTH1. International Journal of Molecular Sciences, 2020, 21, 8860.	4.1	3
43	A comparison of 64Cu-labeled bi-terminally PEGylated A20FMDV2 peptides targeting integrin ανβ6. Oncotarget, 2022, 13, 360-372.	1.8	3
44	Translation of ceragenin affinity for bacteria to an imaging reagent for infection. RSC Advances, 2019, 9, 14472-14476.	3.6	1